

Investigation the Effects of Choking and Combustion Products Swirling Frequency on Fractures of Gas Turbine Compressor Blades

Dr. J. MURALI NAIK

Associate Professor,

Department of Mechanical Engineering,

Holy Mary Institute of Technology and Science,

Bogaram (v), Keesara(m), Medchal Dist, Hyderabad, Telangana-501301

ABSTRACT

Premature blade fractures occurred in four gas turbine compressors at a refinery. To assess the impact of combustion instability on blade failure, such as choking and chamber resonance issues, 3D models of the combustion chamber structure and combustion flow were examined using finite element analysis and computational fluid dynamics codes, respectively. By comparing the natural frequencies of the combustion chamber with the combustion swirl frequency, it was determined that the chamber structure was not experiencing resonance. To verify the likelihood of choking, the Mach number of the combustion product flow was analyzed. The Mach number distribution results indicated that the flow was subsonic in the transition piece area. However, due to the presence of supersonic flow conditions near the swirl vanes, the flow could become supersonic under certain critical conditions. Therefore, it is recommended that operators maintain engine operation as close to the optimal design conditions as possible to avoid choking. The simulation results indicated that the blade fractures were not a result of combustion issues.

Keywords: CFD, fluid instability, turbomachines, reacting flows

1 INTRODUCTION

With the increasing demand for energy, the industrial gas turbine industry has experienced significant growth in recent decades. Design objectives for gas turbines have focused primarily on enhancing efficiency, power density, and overall output. Combustion, which undergoes the greatest entropy change during the power cycle, represents a major source of heat loss. Thus, reducing combustion losses, such as minimizing unburned fuel, is a common approach to improving gas turbine efficiency. One effective method is the use of swirling fuel injection, which enhances the mixing process. However, caution must be exercised when implementing swirling injection to avoid combustion swirl frequencies (CSF) that align with the natural frequencies of the combustion chamber. Such alignment can trigger resonance within the chamber structure, posing serious risks to both turbine and compressor blades. Additionally, the flow instability within the combustion chamber is influenced by factors such as the flow Mach number in the transition piece area and parameters related to detonation dependence. Unfortunately, the presence of unfavorable pressure gradients along the compressor axis can lead to combustion instabilities that may result in stall or, in the worst case scenario, surge problems. Therefore, the design of gas turbine combustion chambers must prioritize safety to prevent unpredictable failures in engine instruments.

There are two distinct aspects in the instability of gas turbine combustion chambers:

Instability of chamber structure can lead to instability of combustion flow and vice versa. Therefore, it is necessary to investigate both structure and combustion flow instabilities in order to demonstrate the instabilities in the combustion chamber. Developing an analytical solution for both aspects of chamber instability is complex due to the variety of engine operating conditions and the complexity of the geometry and boundary conditions that govern it. On the other hand, numerical studies are common and suitable for applying complex boundary conditions to complex geometries. The finite element method can be used to study the instability of combustion structure, while computation fluid dynamics (CFD) codes are more suitable for studying combustion flow instabilities. Combustion flow instabilities in gas turbine engines can be divided into two common distinct parts: choking and detonation. Choking occurs when the flow Mach number in the combustion chamber's exit throat, located in the transition piece, reaches 1. In this situation, the existing acoustic waves push the combustion products into the compressor side, causing a backflow inside it. This is known as choking. When choking occurs, the compressor's performance is disrupted and the reversed flow is seen as a moving pressure wave towards the compressor entrance throat. Detonation, on the other hand, is the instability of the combustion process during the startup operation of the engine. There are suitable engineering studies published in the literature that investigate combustion instabilities in gas turbine combustion chambers. Paxson and Quinn [1] conducted a comprehensive study on the effect of pressure waves on the acoustic modes of the combustion chamber and how it triggers various forms of instability. In addition, Paxson [2] studied the effect of an abrupt change in area in a lean premixed combustor rig and how it accelerates combustion instabilities. Schuermans et al. [3] used numerical tools to model the gas turbine combustion chamber and conducted experiments to observe the response of combustion. Recently, Schmitt et al. [4] examined the interaction of turbulence, acoustics, and combustion in a scaled gas turbine combustor with a single burner.



Fig. 1 Failed blades in first row of four frame-6 gas turbines

Resonance is the other most common and often overlooked instability in gas turbine chambers; it happens when one of the structure's natural frequencies become equal to its CSF. A few papers Several studies have been published addressing this aspect. Caraeni et al. (5) developed a fast method, based on the Arnoldi algorithm, to determine the resonance frequencies of a combustion chamber. More recently, Bethke et al. (6) also determined the resonance frequencies using finite element-based methods. There have been numerous reports of fractures in first-stage moving compressor blades in frame-type gas turbines, including plants in Pakistan, China, Korea, the USA (New Jersey and Newark Bay), and recently in Iran (7). These reports indicate that similar fractures are due to compressor design errors. Conferences have been dedicated to examining the issues with frame-type compressors due to the importance of this

problem (8). In one case, premature fracture of a compressor blade occurred after about 18,000–31,500 hours of operation in four gas turbines at a seaside refinery in Iran (9). As shown in Figure 1, all of the fractures occurred in the first-stage moving blades. It is important to note that all the fractures occurred during normal engine operation, ruling out detonation as a cause. Vibration gauges showed high amplitudes during a brief period of time before accidents. These amplitudes could be attributed to combustion chamber resonance or choking. To determine the probability of chamber resonance, CFD analysis of combustion and finite element modeling of the chamber structure were conducted. These analyses calculated CSF and chamber natural frequencies, respectively. Additionally, the distribution of Mach numbers inside the chamber was studied to determine choking probabilities. The results of these analyses are presented in this paper.

1.1 CASE-STUDIED GAS TURBINES:

Frame-6 gas turbines are composed of 17 stages of compressor disks and 3 stages of turbine disks, as illustrated in Figure 2. The gas turbine's combustion chambers are of the can-annular type, with ten chambers positioned around the rotor between the compressor and turbine sections. These chambers are designed to allow for through-flow, ensuring that the air near the nozzle remains close to the front wall of the liner. The combustion chamber and its arrangement around the turbine rotor can be seen in Figures 3(a) and 3(b), respectively. Air and fuel flow rates, as well as other geometric values that significantly impact chamber instability, are detailed in Section 4.

2. FINITE ELEMENT MODELING

Modal analysis was conducted to determine the vibration mode shapes and natural frequencies of the combustion chamber. A comprehensive 3D model of the combustion chamber, including various components such as the fuel nozzle collar, liner, spring seal, liner stops, liner cap, and transition piece, was created using Solid Works software (Fig. 3(a)). The study then progressed to utilizing the ANSYS finite element code. The resulting finite element model consisted of 121,407 quadratic elements defined in a Cartesian coordinate system. Through modal analysis, the first three natural mode shapes and frequencies were calculated (Fig. 4). It is important to note that the modal analysis solves vibration equations without considering damping ratios. Therefore, the qualitative localized deformations (primarily epicycloids in shape rather than circular) shown in Fig. 4 should be interpreted accordingly. However, the magnitudes of the natural frequencies are precise due to their independence from the damping ratios.

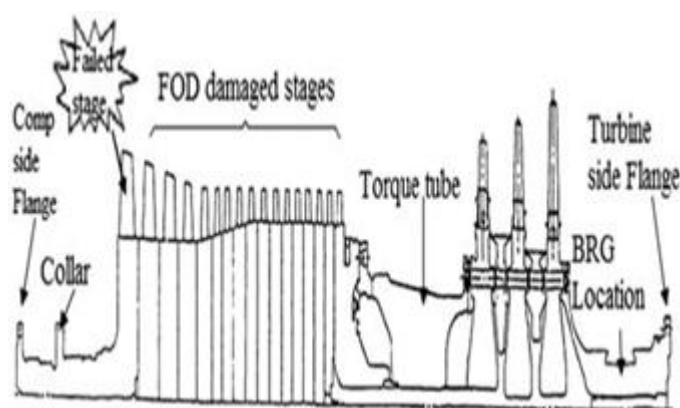


Fig. 2 Side view of the turbine

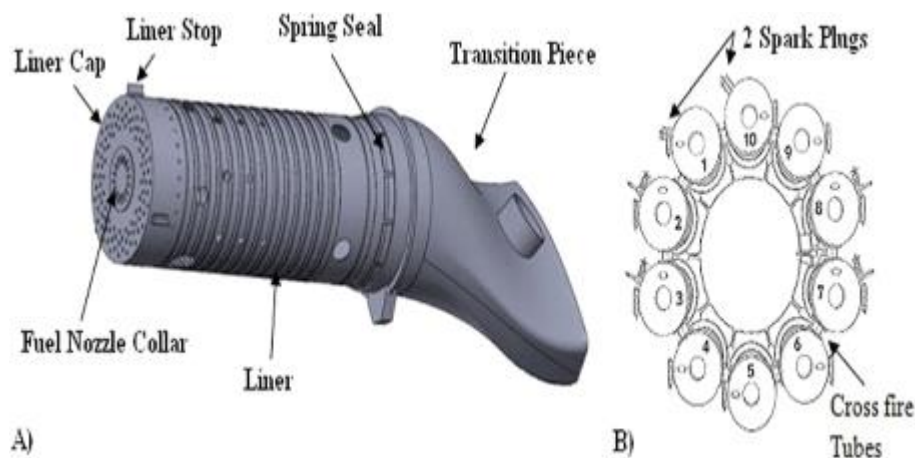


Fig. 3 (a) Schematic of the combustion chamber; (b) arrangement of the chambers on the rotor

Due to the thinness of combustion liners, they are often prone to resonance caused by the swirling flow within the combustion chamber. To mitigate this issue, protective rings are used to enhance chamber stability. However, the use of protective rings in gas turbine combustion chambers significantly increases the risk of resonance in the first three natural modes, which have frequencies of approximately 331, 339, and 369 Hz, respectively.

3. THEORETICAL ANALYSIS OF CSF

When air and fuel are swirled into the combustion chamber, the tangential momentum of the swirling flow generates a tangential shear force on the chamber liner. Consequently, the swirling of combustion products is attributed to the tangential momentum of the swirl vane flows within the chamber, which varies depending on the engine's operating load and condition. As the flow moves towards the chamber outlet, the swirling energy diminishes due to the presence of chamber wall shear stress and the interaction of secondary air inlet flows with the swirling flow.

Therefore, studying the probability of resonance in gas turbine combustion chambers is a crucial issue both in practice and academia. Accordingly, obtaining an accurate analysis of the characteristics of swirling flow aids designers in achieving lower costs and more stable combustion chambers. Theoretical calculations of the characteristics of swirling flow are not suitable due to the complex boundary layers at the chamber walls and the increase in combustion product velocity resulting from combustion reactions. Consequently, numerical analysis must be employed to study swirling flow characteristics increasing combustion product velocity due to combustion reactions; therefore, numerical analysis must be used for it.

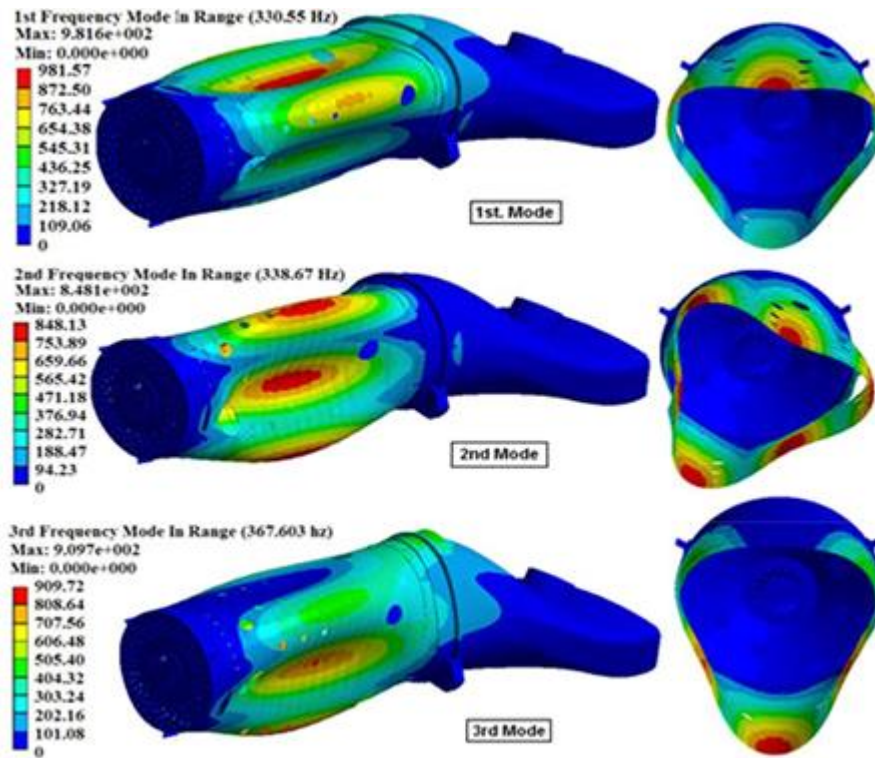


Fig. 4 Three first natural mode shapes and frequencies

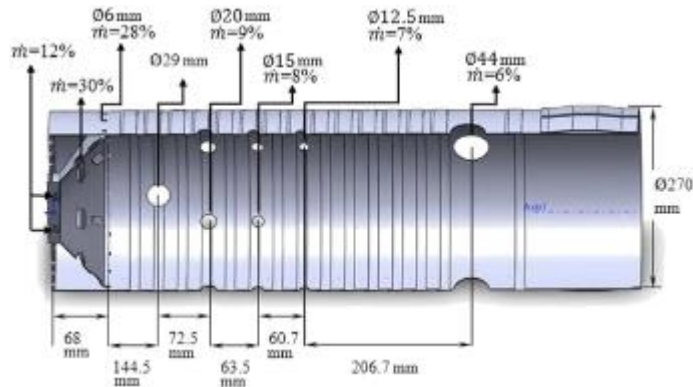


Fig. 5 Air inlet distribution along the combustion chamber

The purpose of theoretical analysis of CSF is to determine and estimate its sources and magnitudes, respectively. The distribution of air flow in the combustion chamber air inlets is shown in Fig. 5. Approximately 7% of the compressor outlet air flow is used for turbine buckets and nozzles cooling, while the remaining 93% enters the combustion chamber. The distribution of this air flow is shown in Fig. 5. Around 58% of the combustion air is used to form an air blanket around the burning gases and dilute the temperature. Of this, 12% enters from swirl vane injectors and 30% enters from the inlets on the conic shape plate (see Fig. 5). The combustion chamber has 16 swirl vanes with an angle of $h_s = 35$ degrees with respect to the tangential coordinate. Figs. 6(a) and 6(b) show the inner view and position of the fuel injectors in the swirl vanes area, respectively. To calculate CSF variations under various engine operation loads, it is necessary to characterize the combustion chamber inlet flow. Figure 7 illustrates the characteristics of the combustion chamber inlet flow in different engine operation loads. Since the combustion fuel momentum is negligible compared to the huge air momentum, its effects on CSF can be ignored under all operating load conditions. The distance of swirl vane tips from the centerline of the

chamber is $R_s = 0.275$ m, and the sum of their areas in each combustion chamber (injector tips area per chamber) is $S_a = 0.0011844$ m². The air velocity of the injectors, V_a , is given by:

$$V_a \approx \frac{\text{Air flow rate}}{S_a} \quad (1)$$

Consequently, CSF can be derived as follows:

$$\text{CSF} \approx \frac{V_a \cos \theta_s}{R_s} = 2\pi R_s \quad (2)$$

CSF was calculated under various engine operation load conditions as shown in Fig. 7. Regarding Fig. 7, as gas turbine operating load increases, the compressor outlet temperature, pressure, and air flow increase. However, CSF, which was calculated from Eq. (2), decreases from 0 to 15 MW and then increases by increasing the operation load. Calculated CSF varies from 80 to 102 (Hz) in miscellaneous operation loads

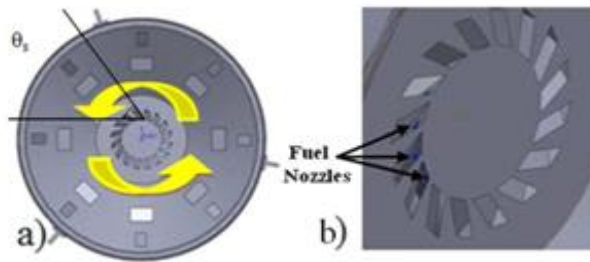


Fig. 6 (a) Chamber inner view of swirl vanes; (b) fuel injectors

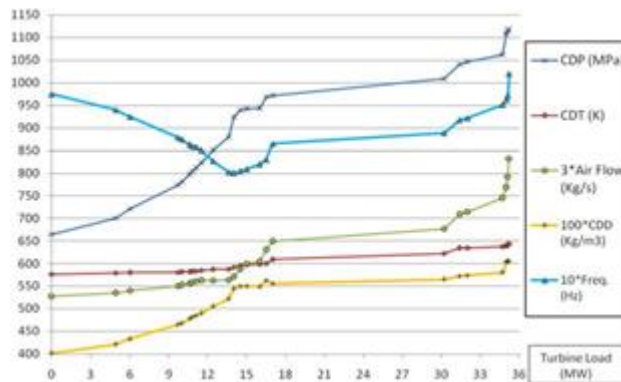


Fig. 7 Characteristics of combustion chamber inlet flow in various operation load of engine

According to calculated natural frequency of chamber structure using ANSYS software and results of theoretical calculated CSF, there is no probability of resonance for the combustion chamber under these conditions. But, as mentioned above, theoretical calculated CSF is not exact and it should be calculated using exact CFD analysis, which is under consideration in Sec.

4. CFD ANALYSI

To demonstrate fuel characteristics, Table 1 shows natural gas characteristics during combustion [10]. A commercial FLUENT soft-ware package [11] was used to simulate combustion, fluid flow, and heat transfer inside the chamber. The constructed chamber ge-ometry was covered with an unstructured hybrid tetrahedral/ wedge by three different meshes (749,983, 883,857 and 1,065,790 cells), and a parametric analysis was accomplished to confirm whether the numerical results were grid-independent or not. After determining mesh independency, the medium-size mesh (883,857 cells) was chosen for the simulations.

Mesh density is refined in the neighborhood of fuel and air inlet sections, being progressively decreased inside the chamber.

Because 14 MW is the most common operating load in South Pars Gas Co. refineries 2 and 3 and all the fractures have occurred under these operating conditions in the aforementioned refineries, it was chosen for the simulation. Furthermore, some arbitrary operating conditions were simulated in order to determine how CSF varies versus various operating loads. The nonpremixed combustion with the PDF model was used to simulate the chamber under these two different operation load conditions.

Table 1 Fuel gas analysis

Analysis SCM: standard cubic meter	Unit	Gas specification limit	Quantity @ 30-Sep-2005
C1	%mol	Min 82	86.67
C2	%mol	Max 12	5.35
C3	%mol	Max 4	1.94
C4	%mol	Max 1	1.00
C5p	%mol	Max 0.4	0.03
CO2	%mol	Max 2	1.30
N2	%mol	Max 5.5	3.71
Gross heating value	MJ/SCM	Min 35.6	37.30
H2S	mg/SCM	Max 4.5	1.68
Total sulphur	mg S/SCM	Max 96.4	22.10
Max captans as sulfur	mg S/SCM	Max 14.2	11.08
Water content	mg/SCM	Max 103	8.00
HC dew point	C	Max 5 C	33 C
		@ 55 barg	@ 85 barg

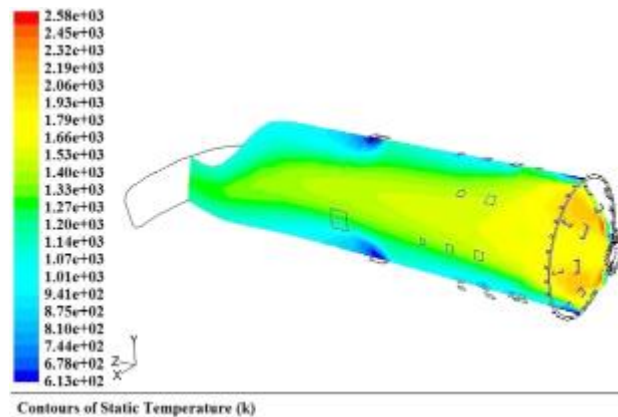


Fig. 8 Contours of temperature in a vertical plane inside the combustion chamber under 14 MW operation.

The velocity, pressure, and temperature fields were calculated by solving the discretized conservation equations for mass fractions, momentum, and energy. The flow was assumed to be stable, and the segregated solver was used because the instability of each conservation equation does not affect the stability of other equations. Turbulence closure was achieved using the standard k-e model [12,13]. The boundary conditions on the inlet sections were fixed for mass flow rates, temperature, and mixture fractions [11]. The liners of the chamber were thermally insulated. The roughness ratio of the walls (ratio of roughness height to the length scale of the geometry) was set at 0.05. The pressure outlet condition was chosen for the outlet boundary, and the gauge pressure was set at 9 bars. The homogeneous combustion gas phase was modeled using the equilibrium hypothesis, while rich flammability limits were applied to evaluate the nonequilibrium reactions as a partial equilibrium model [11].

The instantaneous mass fractions were determined in terms of the instantaneous mixture fraction. Mean mass fractions of fuel, oxidizer, and products were obtained from the mean and variance of instantaneous values, assuming a b-PDF distribution. The SIMPLE method was used for pressure-velocity coupling, and the second-order upwind differential scheme was employed to approximate the convective terms. The solutions were considered converged when the sum of the normalized residuals for each control equation was on the order of 1e-6. The FLUENT 6.3.26 User Manual [11] provides a clear explanation of all the models and procedures used in

the FLUENT software for solving a wide range of fluid mechanics and heat transfer problems. Figure 8 presents contours of temperature for a vertical plane in the chamber under the 14 MW output power condition.

The near-red regions indicate the large amount of heat released by the oxidation of the fuel near the injectors. As the flow moves towards the outlet, the heat is exchanged with the air injected from the liner holes, creating the temperature gradient shown in Fig. 8. The contours of temperature along the length of all the liners of the combustion chamber show that the temperature levels initially increase, reach their maximum, and then decrease. Based on Fig. 8, using swirling vane injectors to create swirling flow in the combustion chamber improves mixing processes and combustion. Figure 9 shows the contours of the Mach number for a vertical plane in the chamber under the 14 MW output power condition.

As shown in Fig. 9, the Mach number of the flow inside the burner is below unity in the transition piece area, indicating subsonic flow in this area.

Regarding Fig. 9, the Mach number is higher in the earlier stages of the chamber. This is because of the significant swirling energy in the flow from the swirl vanes and the intense combustion reaction in this area, resulting in a large swirling momentum. As the flow moves towards the outer part of the chamber, the Mach number decreases as it enters the transition piece area. The increase in the flow Mach number in the transition piece area is due to the specific geometry of this region, which is designed to increase the flow velocity for optimal use in the turbine.

It is important to note that during engine start-up and shut-down, the properties of the combustion flow are more unstable compared to steady operation. Therefore, extra attention should be given to these starting and stopping conditions. To determine the Combustion Stability Factor (CSF), Equation (2) was calculated in the chamber domain. In Figure 10, the contours of CSF are shown for a vertical plane in the chamber under the 14 MW output power condition. As depicted in Figure 10, the CSF near the swirl vanes of the fuel injectors is significantly higher compared to other regions of the chamber. To investigate the effectiveness of CSF, histograms of frequencies were calculated and the results indicated that the 200 Hz frequency covers approximately 70% of the flow very close to the chamber wall. Hence, it is apparent that the effective CSF at the engine's 14 MW output power is approximately 200 Hz. Simulations reveal that the effective CSF ranges from 100 to 250 Hz for various engine operation loads. A comparison of the natural frequencies of the chamber structure with the CSF values (which act as the exiting force frequency) indicates that the chamber design is suitable and there is no risk of resonance occurring during normal engine operation.

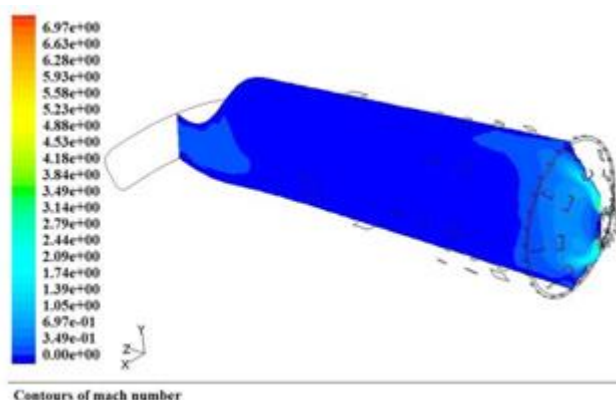


Fig. 9 Contours of Mach number in the combustion chamber under 14 MW operation

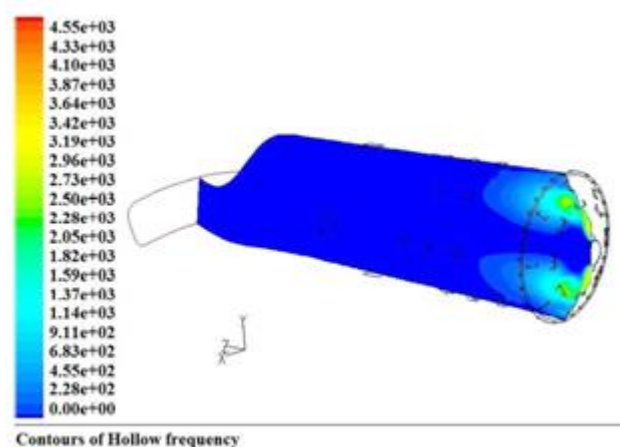


Fig. 10 Contours of hollow frequencies in the combustion chamber under 14 MW operation

5. RESULTS AND CONCLUSIONS

The problem of premature fracture failure of blades occurred in four gas turbine compressors at a refinery. To determine the probability of combustion instability effects on blade failure, a 3D model of the combustion chambers was studied using both finite element (FE) and CFD codes. The distribution of Mach numbers inside the combustion chamber revealed that the flow is subsonic in the transition piece area of the chamber. However, due to the presence of supersonic flow conditions in the earlier stages of the chamber, such as the zones near the swirl vanes, certain unpredictable conditions can lead to supersonic flow in the transition piece area. Additionally, the operation of the combustion chamber during engine start-up is more unstable than during steady load operation, requiring extra attention during these periods.

It was concluded that choking cannot be the cause of compressor blade failure during normal steady operation of these engines. The results of CFD simulations showed that the CSF (combustion stability factor) varies from 100 to 250 Hz during normal operation of a gas turbine. Comparing the natural frequencies of the chamber structure with the CSF revealed that there is no possibility of chamber resonance under the range of operating load conditions. Furthermore, based on the simulation results mentioned above, it can be concluded that the design and manufacturing of this type of combustion chamber are suitable for improving combustion mixing in the chamber.

REFERENCES

1. Quinn, D. D., and Paxson, D. E., 1998, "A Simplified Model for the Investigation of Acoustically Driven Combustion Instabilities," 34th Joint Propulsion Conference, Cleveland, OH, July 12–15.
2. Paxson, D., 2000, "A Sectorized One-Dimensional Model for Simulating Combustion Instabilities in Premix Combustors," 38th Aerospace Sciences Meeting and Exhibit, Reno, NV, Jan. 10–13.
3. Schuermans, B., Bellucci, V., and Paschereit, C. O., 2003, "Thermoacoustic Modeling and Control of Multi Burner Combustion Systems," *ASME*, Paper No. GT2003-38688.
4. Schmitt, P., Poinsot, T., Schuermans, B., and Geigle, K. P., 2007, "Large-Eddy Simulation and Experimental Study of Heat Transfer, Nitric Oxide Emissions and Combustion Instability in a Swirled Turbulent High-Pressure Burner," *J. Fluid Mech.*, 570, pp. 17–46.
5. Caraeni, M. L., Caraeni, D. A., and Fuchs, L., 2003, "Fast Algorithm to Compute Resonance Frequencies of a Combustion Chamber," 9th AIAA/CEAS Aeroacoustics Conference and Exhibit, Hilton Head, SC, May 12–14.
6. Bethke, S., Wever, U., and Krebs, W., 2005, "Stability Analysis of Gas-Turbine Combustion Chamber," 11th AIAA/CEAS Aeroacoustics Conference, Monterey, CA, May 23–25.

7. "R1 Compressor-Blade Failures Dominate Discussion at Annual Meeting," 2007, Combined Cycle Journal, Second Quarter, <http://www.combinedcyclejournal.com/webroot/2Q2007/107,%20p%2072-92%20CTOTF.pdf>
8. "CTOTF Tackles the Tough Issues, Including 7FA R0 and Mid-Compressor Fail-ures," 2007, Combined Cycle Journal, First Quarter, www.combinedcyclejournal.com/webroot/1Q2007/107,%20p%2072-92%20COTF.pdf
9. Poursaeidi, E., Arablu, M., and Mohammadi Arhani, M. R., 2010, "Root Cause Analysis of Unit 2 Refinery Powerplant Gas Turbine Compressors 1st Row Rotating Blade Fractures," South Pars Gas Company, Iran, Technical Report No. 30557.
10. "Process Gas Train Results, Final Results for Export Gas," 2005, Results for UNIT 106SC01, SPGC R&D Center Archives, Iran, Report No. CF2008009.
11. FLUENT Inc., 2007, FLUENT 6.3.26 User Manual.
12. Launder, B. E., and Spalding, D. B., 1972, Lectures in Mathematical Models of Turbulence, Academic, London.
13. Jones, W. P., and Whitelaw, J. H., 1985, "Modeling and Measurements in Turbulent Combustion," *Sym. (Int.) Combust., [Proc.]*, 20(1), pp. 233–249.